Numerical Investigation on Effects of Steel Fibers Content on Flexural Behavior of UHPCC

M. Halimi
M.Sc. Student, Department of Civil Engineering, Faculty of Engineering, Hakim Sabzevari University, Sabzevar, Iran

M. Kioumarsi
Associate Professor, Department of Civil Engineering, Oslo Metropolitan University, Norway

H. Bakhshi
Associate Professor, Department of Civil Engineering, Faculty of Engineering, Hakim Sabzevari University, Sabzevar, Iran

H. Sarkardeh
Assistant Professor, Department of Civil Engineering, Faculty of Engineering, Hakim Sabzevari University, Sabzevar, Iran

ABSTRACT: Ultra-High Performance Cementitious Composites (UHPCC) is a kind of concrete with specific characteristics that has lesser drawbacks in term of tensile strength and breakage. One of the methods for improving the mechanical properties of concrete is adding fibers. This study numerically investigates the effect of steel fiber with different volume fractions (V_f) on flexural behavior of UHPCC using nonlinear finite element method (NLFEM). For this purpose, hooked ended fibers with five different V_f of fibers (0%, 0.5%, 1%, 1.5% and 2%) and aspect ratio length to diameter 80 (L/D=80) are used in four-point bending tests. The modeling of the nonlinear region of three-dimensional (3D) model of concrete is based on concrete damage plasticity model (CDPM). Type and size of the suitable element are chosen based on mesh sensitivity analysis. The interaction mechanism between steel fibers and concrete considered the embedded region algorithm. Finite element modeling of the compressive specimen is validated by comparing the stress-strain curve of the numerical model with that of the experimental study. Results showed that the addition of steel fibers with different V_f caused 6% to 33% improvement in flexural behavior.

1 INTRODUCTION

Ultra-High Performance Cementitious Composites (UHPCC) is a type of building material with ultra-high mechanical properties, dense structure, low capillary porosity and excellent durability (Kioumarsi et al., 2016a, Kioumarsi et al., 2016b). UHPCC has been used extensively throughout the whole world in various structures such as bridge decks, thin shell structures, nuclear power plants and defensive facilities that may experience impact loads during their service life (Rong et al., 2015, Nguyen et al., 2013, Hassan et al., 2012, Farnam et al., 2010, Lai and Sun, 2009). For enhancing the mechanical properties of concrete, numerous researchers (Yoo et al., 2017, Yoo et al., 2015, Yu et al., 2014) have added discontinuous fibers into the concrete mixture that during the last few decades, steel fiber is one of the most widely used (Hao et al., 2016, Hao and Hao, 2013). Effects of fiber shapes, distribution directions and kind of fibers such as hybrid and steel fibers were often explored (NGO and KIM, 2018, Sun et al., 2018, Groeneveld et al., 2018, Wu et al., 2017, Park et al., 2016, Farnam et al., 2010, Habel and Gauvreau, 2008, Lok and Zhao, 2004). Effect of steel fibers in combination with coarse aggregate is investigated on the compressive and flexural toughness of high strength concrete (Jang and Yun, 2018). The results indicated that the mechanical properties of high strength fiber reinforced concrete are volume fraction of aggregate. It is also indicated that the compressive strength and flexural toughness are significantly influenced by the increment in fiber content (Jang and Yun, 2018). Steel fibers with hook ends were recommended to be used for further studies for better workability and were reported to increase the ductility (Holschemacher et al., 2010). In addition, some of researchers are presented the different methods for simulation of steel fiber reinforced concrete and have investigated the role of different characteristics of steel fibers (Fang and Zhang, 2013, Liang and Wu, 2018). Liang et al. (Liang and Wu, 2018) have presented Meso-scale modeling of steel fiber reinforced concrete (SFRC) with high compressive strength, high tensile strength and high flexural strength of SFRC. Fang et al. (Fang and Zhang, 2013) have proposed three-dimensional (3D) modeling of steel fiber reinforced concrete material under intense dynamic loading. Barnett et al. (Barnett et al., 2010) have assessed of fiber orientations in ultra-high performance fiber reinforced concrete. Although many aspects of UHPCC are experimentally investigated, numerically attitude toward understanding the effect of steel fiber with different volume fractions (V_f) is lacking. Nonlinear finite element method (NLFEM) is a suitable practical and economical tool to bridge this gap, especially for analyses of mechanical properties, including

compressive, tensile and flexural behavior of UHPCC.
In this study, effects of five V_f of steel fibers (0%-2%) and aspect ratio length to diameter 80 (L/D=80) on mechanical properties of the UHPCC are investigated. Mechanical properties of the UHPCC specimens are investigated through Nonlinear finite element (NLFE) simulations using the concrete damage plasticity model (CDPM) in ABAQUS software (ABAQUS, 2010). Fibers are distributed with random positions and orientations in the specimens. The interaction mechanism between steel fibers and concrete considered the embedded region algorithm.

2 METHODS AND MATERIALS

2.1 Experimental Data

NLFE analysis, allows simulation of the behavior of reinforced concrete (RC) members with sufficient accuracy in lesser time and cost. In NLFEM, the structure is represented as an assemblage of finite elements, each having well-defined physical and material properties, to obtain the behavior of overall structure (Banjara and Ramanjaneyulu, 2017). In the present research, and as it mentioned before, the numerical simulation of UHPCC was performed using ABAQUS software (ABAQUS, 2010) . In this study, the geometry of the simulated specimens are determined regarding the experiments performed by Ren et al. (Ren et al., 2018), which used four-flexural tests for determination of the flexural behavior of UHPCC. A short-scale specimen for simulation is selected in order to have reduction in time and volume of calculations during the analysis process. As shown in Figure 1, Specimen size in the four-point flexural test is 100×100×400 (mm) with a span length of 300mm.

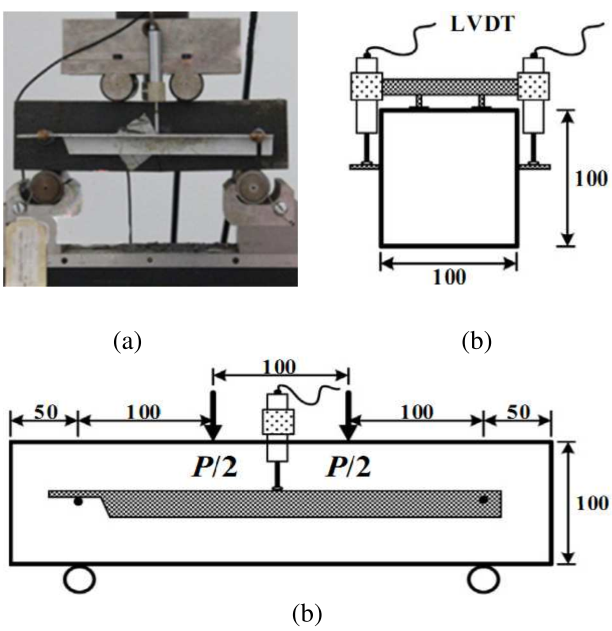

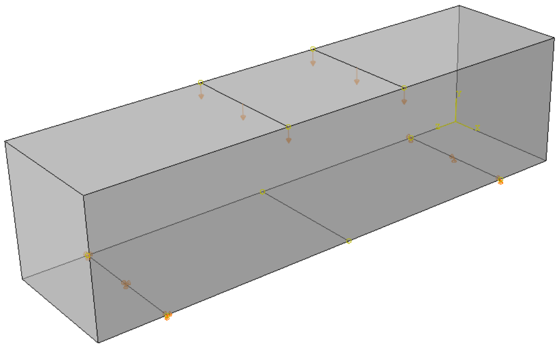
(c)

Figure 1. Four-point flexural test (a) setup (Ren et al., 2018) (b) dimensions of specimen (Ren et al., 2018) (c) NLFE model (unit: mm)

In this experimental test, the concrete material has a compressive strength of 102.2MPa with a modulus of elasticity of 43.7GPa and Poisson's ratio of the concrete material of 0.22. The ingredients of the UHPCC are shown in Table 1.

Table 1. Constituents of UHPCC in the experiments performed by Ren et al. (Ren et al., 2018)

Ingredients	Cement	Silica fume	Ultra-fine mineral admixture	Sand	Water	HRWR*	Fiber content
Weight (kg/m^3)	700	140	110	1200	152	22.8	0-195

* High-range water reducers

Hooked ended steel fibers are used for the UHPCC that is shown in Figure 2. The tensile strength and Young's modulus of the used steel fibers are 1250MPa and 210GPa, respectively (Abbass et al., 2018). Other properties of the used steel fibers are summarized in Table 2.

Figure 2. Geometry of hook ended steel fibers (Ren et al., 2018)

Table 2. Properties of hook ended steel fiber (Abbass et al., 2018).

Length (mm)	Diameter (mm)	(*L/D*)
60	0.75	80

2.2 Numerical model

In this study, steel fibers are simulated with five V_f percentages of fibers: 0%, 0.5%, 1.0%, 1.5% and 2%, with the help of randomly distribution regarding to previous studies (Liang and Wu, 2018, Fang and Zhang, 2013, Barnett et al., 2010). The model with $V_f = 1\%$ is shown in Figure 3.

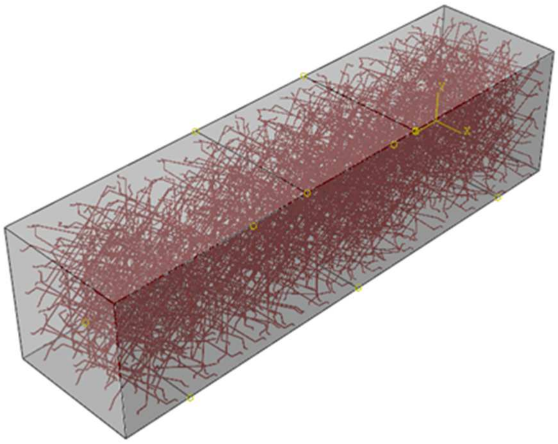

(a)

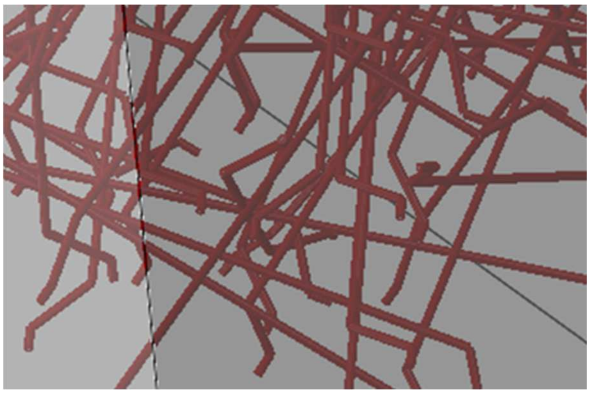

(b)

Figure 3. NLFE model with 1% volume fractions (V_f) of fibers with randomly distributed fibers with different viewing angle: (a) perspective (b) close up

To express the elastic-plastic behavior of RC, the CDPM is assumed as a constitutive model of concrete material (Kmiecik and Kamiński, 2011, Lee and Fenves, 1998, Lubliner et al., 1989). The CDPM (ABAQUS, 2010) is a continuum, plasticity-based, damage model for concrete. It assumes that the main two failure mechanisms are tensile cracking and compressive crushing of the concrete material. The yield surface is controlled by two variables representing equivalent plasticity strains: $\tilde{\varepsilon}_t^{pl}$ and $\tilde{\varepsilon}_c^{pl}$, associated with failure mechanisms under tensile and compressive loading, respectively. The degradation of the elastic stiffness is represented by two different damage variables: d_t for tension and d_c for compression. These variables are calculated by equivalent plasticity strains. They can take values from 0–which represents undamaged material–to 1, which represents a total loss of strength. The post-failure stresses in tension (t) and compression (c) are given by Equations 1-2:

$$\sigma_t = (1 - d_t)\left(\varepsilon_t - \tilde{\varepsilon}_t^{pl}\right)E_0 \quad (1)$$

$$\sigma_c = (1 - d_c)\left(\varepsilon_c - \tilde{\varepsilon}_c^{pl}\right)E_0 \quad (2)$$

where σ_t and σ_c are post-failure stresses in tension and compression. E_0 is the original stiffness of the material. Variables ε_t and ε_c are the strains in tension and compression, respectively. Also, variables $\tilde{\varepsilon}_t^{pl}$ and $\tilde{\varepsilon}_c^{pl}$ are the equivalent plastic strains in tension and compression, respectively. The model needs numerical values of post-failure stress and damage with cracking strain $\tilde{\varepsilon}_t^{ck}$ and inelastic strain $\tilde{\varepsilon}_c^{in}$ for tension and compression. The cracking and inelastic strains are calculated by the following Equations:

$$\tilde{\varepsilon}_t^{ck} = \varepsilon_t - \varepsilon_{0t}^{el} \quad (3)$$

$$\tilde{\varepsilon}_c^{in} = \varepsilon_t - \varepsilon_{0c}^{el} \quad (4)$$

where $\varepsilon_{0t}^{el} = \sigma_t/E_0$, $\varepsilon_{0c}^{el}=\sigma_c/E_0$ are the elastic tensile and compressive strain of the concrete, respectively. ABAQUS converts the cracking strain and the inelastic strain values to plastic strain values using the relationship:

$$\tilde{\varepsilon}_t^{pl} = \tilde{\varepsilon}_t^{ck} - \frac{d_t\sigma_t}{(1 - d_t)E_0} \quad (5)$$

$$\tilde{\varepsilon}_c^{pl} = \tilde{\varepsilon}_c^{ck} - \frac{d_t\sigma_c}{(1 - d_c)E_0} \quad (6)$$

For the mesh sensitivity analysis and validation of NLFE modeling, compressive strength test is used. The accuracy of results depends significantly mesh. In this paper, the 8-noded hexahedral (brick) element incorporated with reduced integration is used for representing concrete (Liu et al., 2017). This element is capable of plastic deformation and cracking in three orthogonal directions at each integration point. 2-node linear 3D truss element is used for steel fibers. This element is described by two nodes and three degrees of freedom at each node (Larbi et al., 2013).

2.2.1 Mesh sensitivity analysis

The accuracy of results depends on mesh density. Trial analysis is carried out by varying the mesh size in order to obtain the optimum mesh density. In this study, four trial analysis are carried out using mesh sizes 6.25, 12.5, 25 and 50mm. Figure 4 shows the plot of mesh size versus stress-strain curve which shows a little variation of compressive strength with respect to the mesh size from 12.5 to 6.25mm. Hence, an optimum mesh size of 12.5mm is adopted for further numerical investigations in this study.

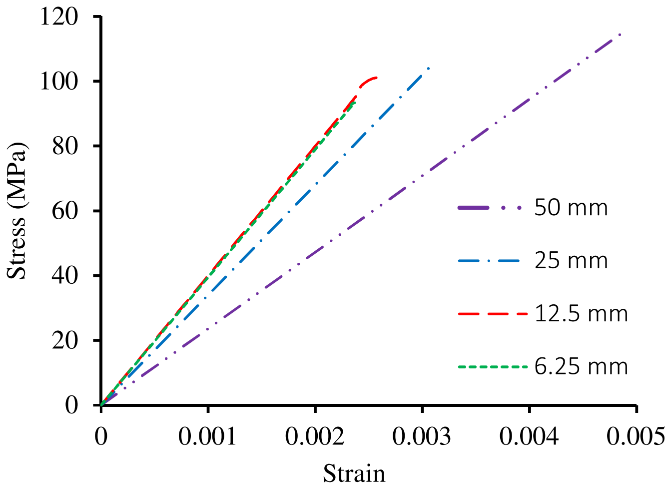

Figure 4. Influence of mesh density on compressive strength.

2.2.2 *Validation of the NLFE model*

NLFE modeling of the compressive specimen is validated by comparing the stress-strain curve of the numerical model with that of the experimental study as shown in Figure 5. Very good agreement is observed in the experimental study with that obtained results from the finite element analysis. Thus, it could be concluded that the NLFE models are valid and reliable to be used as a valid numerical tool to investigate the performance of specimens strengthened with steel fibers.

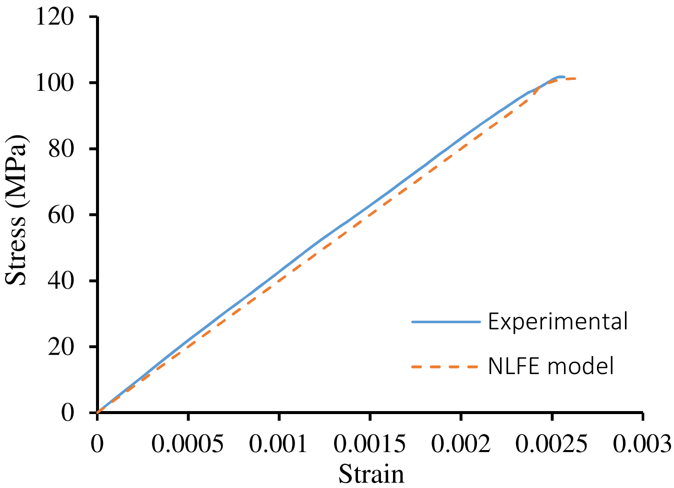

Figure 5.Validation of the NLFE model

3 RESULTS AND DISCUSSIONS

In this section, how steel fibers, including different V_f and L/D=80, affect properties of UHPCC are investigated based on the validated NLFE models. Specimens with various V_f are numerically studied to investigate the relationship between V_f and the flexural behavior of UHPCC. Load-deflection curves under V_f are illustrated in Figure 6. As it can be seen, the addition of the steel fibers has influenced the four-point flexural load-deflection curves of UHPCC. It can be seen that deflection hardening is appeared and enhanced by increasing the V_f. In addition, the effects of V_f on the maximum flexural load of UHPCC and volume of improvement of maximum load are represented in Figure 7 and 8, respectively. It indicates that, addition of steel fibers has favorable effect on improving the maximum flexural load. Table 5 lists the maximum flexural load under various fiber contents.

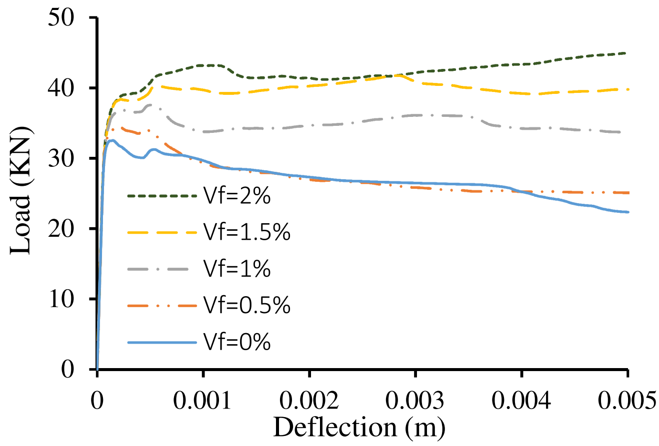

Figure 6. Representative four-point flexural load-deflection curves of UHPCC under different V_f

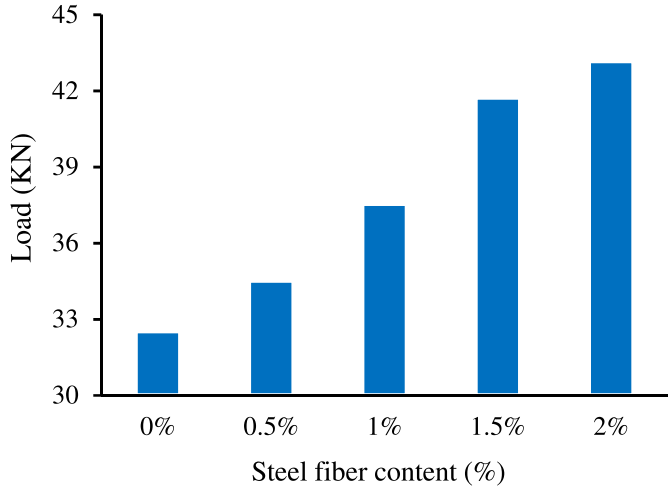

Figure 7. Effects of V_f on the maximum flexural load

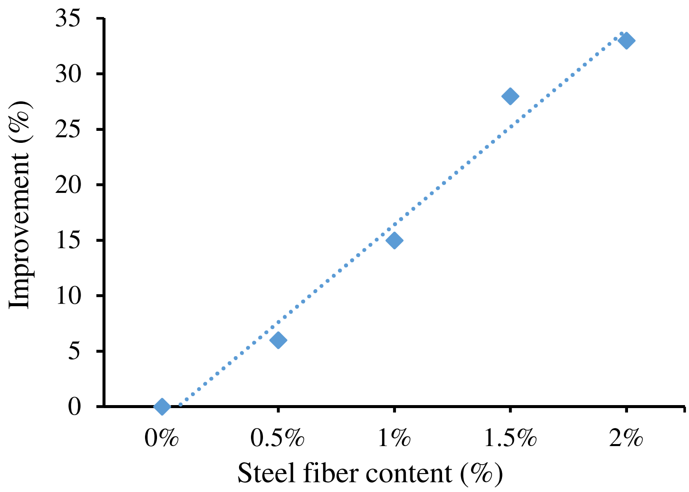

Figure 8. Effects of V_f on the volume of improvement of maximum flexural load

As shown in Figure 7 and 8, by addition of steel fiber to the UHPCC, its flexural behavior improves. For 0.5% content of V_f, the maximum load is increased up to 6%. At V_f of 1% and 1.5%, the maximum loads reached 15% and 28%, which represent the growth of 9% and 13% compared to previous one, respectively. Furthermore, for 2% content of V_f, the increment reached to top of 33%.

Table 1. Maximum load under different V_f.

	Fiber content (by volume)				
Aspect ratio	0%	0.5%	1%	1.5%	2%
80	32544	34538	37564	41745	43187

4 CONCLUSIONS

In this study, Simulations of four-point flexure are conducted so that investigate the effects of steel fiber with different V_f flexural behavior of UHPCC. The following conclusions can be drawn:

(1) Good agreement between the measured experimental data and predicted results of NLFE models is observed.
For the four-point flexural properties of UHPCC, with the increase of steel fiber content, the behavior of four-point flexural load-deflection curves turns to be deflection hardening. Moreover, addition of steel fibers has favorable effect on improving the flexural behavior.

(2) For 0.5% content of V_f, the maximum load is increased up to 6%. At V_f of 1% and 1.5%, the maximum loads reached 15% and 28%, which represent the growth of 9% and 13% compared to previous one, respectively. Furthermore, for 2% content of V_f, the increment reached to top of 33%.

List of symbols

D	Diameter
L	Length
V_f	Volume of fraction
σ_t	Post-failure stresses in tension
σ_c	Post-failure stresses in compression
d_t	Damage variable in tension
d_c	Damage variable in compression
ε_t	Strain in tension
ε_c	Strain in compression
$\tilde{\varepsilon}_t^{pl}$	Equivalent plastic strains in tension
$\tilde{\varepsilon}_c^{pl}$	Equivalent plastic strains in compression
E_0	Initial elastic stiffness
$\tilde{\varepsilon}_t^{ck}$	Cracking strain in tension
$\tilde{\varepsilon}_c^{in}$	Inelastic strain in compression
ε_{0t}^{el}	Elastic strain in tension corresponding to the undamaged material
ε_{0c}^{el}	Elastic strain in compression corresponding to the undamaged material

REFERENCES

Abaqus (2010) *Abaqus Analysis User's Manual.*

Abbass, W., Khan, M. I. & Mourad, S. (2018) Evaluation of mechanical properties of steel fiber reinforced concrete with different strengths of concrete. *Construction and Building Materials* 168:556-569.

Banjara, N. K. & Ramanjaneyulu, K. (2017) Experimental and numerical investigations on the performance evaluation of shear deficient and GFRP strengthened reinforced concrete beams. *Construction and Building Materials* 137:520-534.

Barnett, S. J., Lataste, J.-F., Parry, T., Millard, S. G. & Soutsos, M. N. (2010) Assessment of fibre orientation in ultra high performance fibre reinforced concrete and its effect on flexural strength. *Materials and Structures* 43(7):1009-1023.

Fang, Q. & Zhang, J. (2013) Three-dimensional modelling of steel fiber reinforced concrete material under intense dynamic loading. *Construction and Building Materials* 44:118-132.

Farnam, Y., Mohammadi, S. & Shekarchi, M. (2010) Experimental and numerical investigations of low velocity impact behavior of high-performance fiber-reinforced cement based composite. *International Journal of Impact Engineering* 37(2):220-229.

Groeneveld, A. B., Ahlborn, T. M., Crane, C. K., Burchfield, C. A. & Landis, E. N. (2018) Dynamic strength and ductility of ultra-high performance concrete with flow-induced fiber alignment. *International Journal of Impact Engineering* 111:37-45.

Habel, K. & Gauvreau, P. (2008) Response of ultra-high performance fiber reinforced concrete (UHPFRC) to impact and static loading. *Cement and Concrete Composites* 30(10):938-946.

Hao, Y. & Hao, H. (2013) Dynamic compressive behaviour of spiral steel fibre reinforced concrete in split Hopkinson pressure bar tests. *Construction and Building Materials* 48:521-532.

Hao, Y., Hao, H. & Chen, G. (2016) Experimental investigation of the behaviour of spiral steel fibre reinforced concrete beams subjected to drop-weight impact loads. *Materials and Structures* 49(1-2):353-370.

Hassan, A., Jones, S. & Mahmud, G. (2012) Experimental test methods to determine the uniaxial tensile and compressive behaviour of ultra high performance fibre reinforced concrete (UHPFRC). *Construction and Building Materials* 37:874-882.

Holschemacher, K., Mueller, T. & Ribakov, Y. (2010) Effect of steel fibres on mechanical properties of high-strength concrete. *Materials & Design (1980-2015)* 31(5):2604-2615.

Jang, S.-J. & Yun, H.-D. (2018) Combined effects of steel fiber and coarse aggregate size on the compressive and flexural toughness of high-strength concrete. *Composite Structures* 185:203-211.

Kioumarsi, M., Parsa, E., Sharbatdar, M. K., Kheyroddin, A. & Markeset, G. (2016a) Ductility and structural characteristics of damaged RC frames strengthened with HPFRCC layer. *Nordic Concrete Research* 55.

Kioumarsi, M., Tajfar, M., Kheyroddin, A. & Kioumarsi, B. (2016b) Investigation of the seismic response of reinforced concrete column-beam connections using high performance fibre reinforced cementitious composites (HPFRCC). *Nordic Concrete Research* 55.

Kmiecik, P. & Kamiński, M. (2011) Modelling of reinforced concrete structures and composite structures with concrete strength degradation taken into consideration. *Archives of civil and mechanical engineering* 11(3):623-636.

Lai, J. & Sun, W. (2009) Dynamic behaviour and visco-elastic damage model of ultra-high performance cementitious composite. *Cement and Concrete Research* 39(11):1044-1051.

Larbi, A. S., Agbossou, A. & Hamelin, P. (2013) Experimental and numerical investigations about textile-reinforced concrete and hybrid solutions for repairing and/or strengthening reinforced concrete beams. *Composite Structures* 99:152-162.

Lee, J. & Fenves, G. L. (1998) A plastic-damage concrete model for earthquake analysis of dams. *Earthquake engineering & structural dynamics* 27(9):937-956.

Liang, X. & Wu, C. (2018) Meso-scale modelling of steel fibre reinforced concrete with high strength. *Construction and Building Materials* 165:187-198.

Liu, K., Xie, H., Jin, C., Huang, S. & Wang, F. (2017) The equivalent plasticity strain analysis of snow-melting heated pavement concrete exposed to inner elevated temperatures. *Construction and Building Materials* 137:66-75.

Lok, T. & Zhao, P. (2004) Impact response of steel fiber-reinforced concrete using a split Hopkinson pressure bar. *Journal of Materials in Civil Engineering* 16(1):54-59.

Lubliner, J., Oliver, J., Oller, S. & Onate, E. (1989) A plastic-damage model for concrete. *International Journal of solids and structures* 25(3):299-326.

Ngo, T. T. & Kim, D. J. (2018) Shear stress versus strain responses of ultra-high-performance fiber-reinforced concretes at high strain rates. *International Journal of Impact Engineering* 111:187-198.

Nguyen, D. L., Kim, D. J., Ryu, G. S. & Koh, K. T. (2013) Size effect on flexural behavior of ultra-high-performance hybrid fiber-reinforced concrete. *Composites Part B: Engineering* 45(1):1104-1116.

Park, S. H., Kim, D. J. & Kim, S. W. (2016) Investigating the impact resistance of ultra-high-performance fiber-reinforced concrete using an improved strain energy impact test machine. *Construction and Building Materials* 125:145-159.

Ren, G., Wu, H., Fang, Q. & Liu, J. (2018) Effects of steel fiber content and type on static mechanical properties of UHPCC. *Construction and Building Materials* 163:826-839.

Rong, Z., Sun, W., Xiao, H. & Jiang, G. (2015) Effects of nano-SiO2 particles on the mechanical and microstructural properties of ultra-high performance cementitious composites. *Cement and Concrete Composites* 56:25-31.

Sun, X., Zhao, K., Li, Y., Huang, R., Ye, Z., Zhang, Y. & Ma, J. (2018) A study of strain-rate effect and fiber reinforcement effect on dynamic behavior of steel fiber-reinforced concrete. *Construction and Building Materials* 158:657-669.

Wu, Z., Shi, C., He, W. & Wang, D. (2017) Static and dynamic compressive properties of ultra-high performance concrete (UHPC) with hybrid steel fiber reinforcements. *Cement and Concrete Composites* 79:148-157.

Yoo, D.-Y., Banthia, N., Kim, S.-W. & Yoon, Y.-S. (2015) Response of ultra-high-performance fiber-reinforced concrete beams with continuous steel reinforcement subjected to low-velocity impact loading. *Composite Structures* 126:233-245.

Yoo, D.-Y., Banthia, N. & Yoon, Y.-S. (2017) Impact resistance of reinforced ultra-high-performance concrete beams with different steel fibers. *ACI Structural Journal* 114(1):113.

Yu, R., Spiesz, P. & Brouwers, H. (2014) Static properties and impact resistance of a green Ultra-High Performance Hybrid Fibre Reinforced Concrete (UHPHFRC): experiments and modeling. *Construction and Building Materials* 68:158-171.